Soft Matter

Accepted Manuscript

Foam drainage placed on a porous substrate

O. Arjmandi-Tash[1], N. Kovalchuk[1,2], A. Trybala[1], V. Starov[1]

[1]Department of Chemical Engineering, Loughborough University, UK

[2]Institute of Biocolloid Chemistry, Kiev, Ukraine

Graphical Abstract

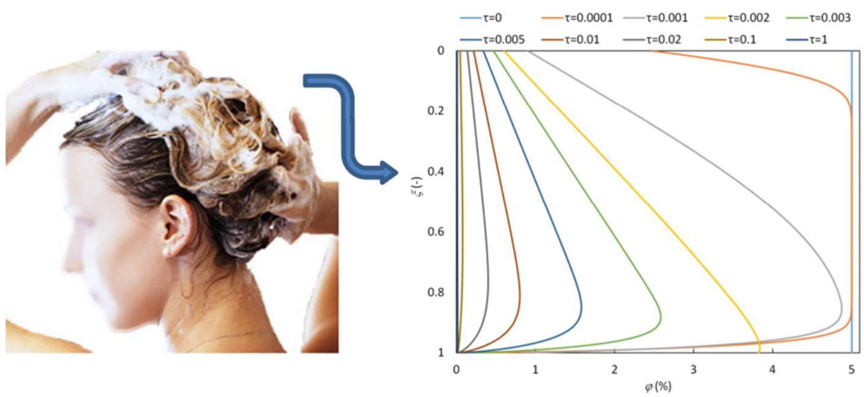

Direct numerical simulations were performed to identify the kinetics of liquid release from a foam into a porous substrate like a skin or a bunch of hair.

Corresponding Author: Victor Starov, Department of Chemical Engineering, Loughborough University, Loughborough, LE113TU, UK. E-mail: V.M.Starov@lboro.ac.uk

Abstract

A model for drainage/imbibition of a foam placed on the top of a porous substrate is presented. The equation of liquid imbibition into the porous substrate is coupled with foam drainage equation at the foam/porous substrate interface. The deduced dimensionless equations are solved using finite element method. It was found that the kinetics of foam drainage/imbibition depends on three dimensionless numbers and initial liquid volume fraction. The result shows that there are three different regimes of the process. Each regime starts after initial rapid decrease of a liquid volume fraction at the foam/porous substrate interface: (i) *rapid imbibition*: the liquid volume fraction inside the foam at foam/porous substrate interface remains constant close to a final liquid volume fraction; (ii) *intermediate imbibition*: the liquid volume fraction at the interface with porous substrate experiences a peak point and imbibition into the porous substrate is slower as compared with the drainage; (iii) *slow imbibition*: the liquid volume fraction at foam/porous substrate interface increases to a maximum limiting value and a free liquid layer is formed between the foam and the porous substrate. However, the free liquid layer disappears after some time. The transition points between these three different drainage/imbibition regimes were delineated by introducing two dimensionless numbers.

1 Introduction

Foams are multiphase colloidal systems, which are formed by trapping a gas in a continuous phase (liquid or a solid). Foams are widely used in personal care products and they often arise during cleaning and dispensing processes. They pop up in lightweight mechanical materials and affect absorbing components in cars, heat exchangers and textured wallpapers. Foams are widely utilised in food, cosmetics, pharmacy, mining, petroleum and gas industries.[1-3] That is why they attract scientific attention already over many decades.[4-10]

The liquid flow in between the gas bubbles through Plateau borders, nodes and films in foam driven by capillarity and/or gravity forces is referred to as drainage. The equations of foam drainage were derived using the combination of the liquid momentum and mass balance equations. The drainage equations have been solved numerically and/or analytically for various situations including free drainage, where liquid drains out of a foam due to the influence of gravity and capillarity,[11-16] wetting of a dry foam, where a dry foam is in contact with a liquid at its base and the liquid rises to the top by capillarity,[17, 18] forced drainage, where liquid is added to the top of foam column producing a traveling wave,[15, 16, 19-21] and pulsed drainage, where a small volume of liquid is injected at the top of a foam and left to evolve.[15, 22-24] A especial case of these situations is the gravity-free case, where a liquid flows in a foam in the absence of significant gravitational forces and the motion of the liquid is governed by the capillarity only.[17, 25, 26]

The studies on drainage kinetics are of a significant importance for industry. Accordingly, theories of foam drainage have been developed over the last decades [22, 27] and a number of techniques and methods such as foam pressure drop technique,[1] Eiffel Tower construction,[28] and Plateau border apparatus experiment [29] have been proposed to control and/or accelerate the rate of liquid drainage. The rate of liquid drainage in these techniques can be adjusted by a controlled reduction of the pressure at the top and/or at the bottom of the foam column, by varying the shape and geometry of the container, and by changing the surface properties of the foaming solution, respectively. Despite a considerable progress in controlling the rate of foam drainage and understanding foam properties, there is still no straightforward way to create foam with desirable properties suitable for a specific application.

Recent investigations have confirmed that foams are an efficient alternative method of drug delivery on the skin of patients.[30-33] Lotions, creams, gels and ointment are the most common topical vehicle delivery systems that have been applied in dermatology; foams are delivery systems which grow in popularity. The density of foams is much lower than that of traditional vehicles and they spread out more easily.[3] This reduces the requirement of applying pressure or prolonged period of contact with the sensitive diseased skin.[31] In addition, drugs from foams absorb and penetrate more quickly as compared to other carriers. The rate of drug delivery from foams can be controlled by the rate of foam drainage and collapse. Kinetics of topical drug delivery can be tailored by varying such foam characteristics as the bubbles size, liquid viscosity, initial liquid content and surface tension. In order to make a proper choice of foam characteristics, processes of drug delivery from foam should be considered in connection with the properties of substrate where the foam is applied to (skin or hair). Skin or bunch of hair have porous structure of their own, therefore an additional phenomenon, a capillary suction into porous substrate affects the foam drainage/imbibition.

Analysis of liquid drainage and flow in foams confined in porous media has been widely investigated in literature [10, 34-39] from both theoretical and experimental points of view. However, a theoretical description of foam drainage/imbibition in contact with a porous substrate (i.e. a foam placed on the top of a porous substrate), which is applicable to the analysis of liquid release from foam into skin or bunch of hair, has been introduced only recently in [40]. It was found that the kinetics of foam drainage/imbibition depends on three dimensionless numbers. The aim of the present study is to develop computer simulations of the drainage/imbibition of foam placed on porous substrate and to investigate different regimes of this process. The effect of all dimensionless numbers on the kinetics of liquid release from foam into porous substrate is investigated and transition points between different drainage/imbibition regimes are found.

2 Mathematical model

There is a substantial difference in the drainage/imbibition of foam in the case of a free drainage (for example, foam placed on a solid substrate) and a drainage/imbibition of a foam placed on a porous substrate. In both cases the drainage is caused by the action of both gravity and the capillary forces. However, if foam is initially wet enough, then sooner or later the drainage/imbibition results in a formation of a free water layer under the foam and the water content in the foam layer immediately above the free water layer reaches the rigidity limit [41] which for 3D mono-disperse foam can be estimated as 0.36 corresponding to random packing limit for spherical particles.[42] Sometimes the maximum liquid fraction is estimated as 0.26, what correspond to the minimum possible voids content at hexagonal packing of equal spheres.[4] The latter value is accepted below. The equilibrium distribution of the water contents in the foam in the end of a free drainage is well known.[4, 15] Important to notice that even in a relatively thin foam layer, the water content distribution is non-uniform over the foam height: from the highest possible at the bottom to the lowest at the top.

The scenario is substantially different in the case of foam placed on a porous substrate: (i) the presence of unsaturated pores inside the porous layer results in an imbibition of water from the Plateau channels into the pores, i.e. drainage/imbibition proceeds faster and (ii) this results in a drier foam layer in contact with a porous substrate and close to the end of the drainage/imbibition process the liquid volume fraction will become lower as compared with the free drainage and below some final value. The final value can be characterised as follows: if the water contents is above this final value then the pressure inside the Plateau channels is positive, that is, the liquid will flow from the Plateau channels to outside. If the final value of the water content is reached then by further drainage the pressure inside the Plateau channels becomes smaller than the capillary pressure inside the pores of the porous substrate and the drainage stops. The previous consideration shows that the final equilibrium distribution of water content over the foam height is lower in the case of drainage/imbibition in contact with the porous substrate than in the case of a free drainage over a non-porous substrate.

2.1 Flow inside foam

Let us consider a foam composed of bubbles of uniform size placed on a horizontal porous substrate. Drainage occurs in the vertical direction along the co-ordinate axis z directed downward, with z=0 at the top of the foam. It is assumed also that the bubble size remains constant during the drainage. Below we use the model of Plateau borders mediated foam drainage where the dissipation in the nodes is neglected. In this case the drainage kinetics can be described by the following equation:[15]

$$\frac{\partial A}{\partial t}+\frac{\partial}{\partial z}\left[\frac{1}{3\mu f}\left(\rho g A^2 - C\gamma\frac{\sqrt{A}}{2}\frac{\partial A}{\partial z}\right)\right]=0\,, \qquad (1)$$

where μ is the dynamic viscosity of liquid, which foam is built of, $f\sim 49$, $A(z, t)$ is the Plateau border cross-section at position z and time t; ρ and g are the liquid density and the gravity acceleration, respectively; $C^2=\sqrt{3}-\pi/2 \sim 0.161$, and γ is the liquid-air interfacial tension. In Eq. (1) the first term in parentheses describes the contribution of the gravitation and the second term is the contribution of the capillary forces to the drainage.

According to [4]

$$R_{pb} = R_b \sqrt{\frac{\varphi C_1}{C^2}} \tag{2}$$

or

$$A = C_1 \varphi R_b^2 , \tag{3}$$

where R_b and R_{pb} are the radii of the bubble and Plateau border, respectively, φ is liquid volume fraction and C_1 is a geometrical coefficient, C_1~0.4857 for a foam with Kelvin structure.[4]

Substitution of Eq. (3) into Eq. (1) results in the following equation for the liquid volume fraction φ:

$$\frac{\partial \varphi}{\partial t} + \frac{\partial}{\partial z}\left(\frac{C_1 \rho g R_b^2}{3\mu f}\varphi^2 - \frac{C\sqrt{C_1}\gamma R_b}{6\mu f}\sqrt{\varphi}\frac{\partial \varphi}{\partial z} \right) = 0 . \tag{4}$$

Let us introduce the following dimensionless variable and co-ordinate: $\zeta \to z/H,\quad \tau \to t/t_0,\quad \phi \to \varphi/\varphi_{cr}$, where H is the foam height, t_0 is the time scale of the process to be determined below and φ_{cr} is the liquid volume fraction after the pressure inside the Plateau channels and the pressure inside the porous substrate equilibrate. Substitution of these variables into Eq. (4) results in

$$\frac{\partial \phi}{\partial \tau} + \frac{\partial}{\partial \zeta}\left(\frac{t_0 C_1 \rho g R_b^2 \varphi_{cr}}{3\mu f H}\phi^2 - \frac{t_0 C\sqrt{C_1}\gamma R_b \sqrt{\varphi_{cr}}}{6\mu f H^2}\sqrt{\phi}\frac{\partial \phi}{\partial \zeta} \right) = 0 , \tag{5}$$

There are two dimensionless parameters in the latter equation. Their ratio is $\frac{t_0 C_1 \rho g R_b^2 \varphi_{cr}}{3\mu f H} / \frac{t_0 C\sqrt{C_1}\gamma R_b \sqrt{\varphi_{cr}}}{6\mu f H^2} = \frac{2\rho g R_b H \sqrt{C_1}}{C\gamma}\sqrt{\varphi_{cr}}$. The latter means that if we select the characteristic time scale from the following condition: $\frac{t_0 C\sqrt{C_1}\gamma R_b \sqrt{\varphi_{cr}}}{6\mu f H^2} = 1$, then:

$$t_0 = \frac{6\mu f H^2}{C\sqrt{C_1}\gamma R_b \sqrt{\varphi_{cr}}} , \tag{6}$$

Substitution of Eq. (6) into Eq. (5) results in

$$\frac{\partial \phi}{\partial \tau}+\frac{\partial}{\partial \zeta}\left(\frac{2\rho g R_b H\sqrt{C_1}}{C\gamma}\sqrt{\varphi_{cr}}\,\phi^2-\sqrt{\phi}\,\frac{\partial \phi}{\partial \zeta}\right)=0\,. \tag{7}$$

Assuming that the liquid films between bubbles in foam are flat (i.e. in a dry foam, R_b>> R_{pb}) the pressure in all bubbles is identical [43] and equals to:

$$P_b = P_a + \frac{4\gamma}{R_b}, \tag{8}$$

where P_a is the atmospheric pressure. The pressure in the Plateau border is lower than that in the bubbles on the value of the capillary pressure: [43]

$$P_c = \frac{\gamma}{R_{pb}}, \tag{9}$$

From Eqs. (2), (8) and (9) the pressure in the Plateau border is

$$P_{pb}(z,t) = P_a + \frac{\gamma}{R_b}\left(4-\frac{C}{\sqrt{C_1\varphi(z,t)}}\right). \tag{10}$$

Let us introduce P_{pm} as the mean capillary pressure inside capillaries in the porous substrate, which can be estimated by $P_{pm} \sim n\gamma/R_{pm}$, where R_{pm} is radius of pores, n =1 in the case of porous media built by cylinders and n=2 in the case of two dimensional geometry. Accordingly, the pressure difference, which results in the liquid flow from the Plateau channel into the porous substrate at the foam/porous substrate interface, will be

$$\Delta P = P_{pb} - P_{pm} = \frac{\gamma}{R_b}\left(4-\frac{C}{\sqrt{C_1\varphi(z=H,t)}}\right)+\frac{n\gamma}{R_{pm}}\,. \tag{11}$$

If ΔP > 0, then liquid from the Plateau border will penetrate into the porous substrate. If ΔP < 0, then penetration will not happen. The latter consideration and Eq. (11) determine the final liquid content, when ΔP=0:

$$\frac{\gamma}{R_b}\left(4-\frac{C}{\sqrt{C_1\varphi_{cr}}}\right)+\frac{n\gamma}{R_{pm}}=0 \tag{12}$$

Hence,

$$\varphi_{cr}=\frac{\left(\frac{C^2}{16C_1}\right)}{\left(1+\frac{nR_b}{4R_{pm}}\right)^2} \tag{13}$$

If we introduce α as a ratio of capillary pressure in the porous substrate to capillary pressure in the bubbles:

$$\alpha=\frac{\Delta P_{\text{cap in substrate}}}{\Delta P_{\text{cap in bubbles}}}=\frac{\frac{n\gamma}{R_{pm}}}{\frac{4\gamma}{R_b}}=\frac{nR_b}{4R_{pm}}, \tag{14}$$

then, Eq. (13) can be rewritten as:

$$\varphi_{cr}=\frac{\left(\frac{C^2}{16C_1}\right)}{(1+\alpha)^2} \tag{15}$$

Substitution of expression (13) into Eq. (6) results in the following expression for the characteristic time of the foam drainage:

$$t_0=\frac{6\mu fH^2}{C^2\gamma}\left(\frac{4}{R_b}+\frac{n}{R_{pm}}\right). \tag{16}$$

If we introduce Bond number as a ratio of hydrostatic pressure in foam to capillary pressure in bubbles:

$$Bo=\frac{\Delta p_{grav}}{\Delta p_{cap}}=\frac{\rho gH}{\frac{4\gamma}{R_b}}, \tag{17}$$

then substitution of Eq. (13) into Eq. (7) results in the following dimensionless equation for the foam drainage:

$$\frac{\partial\phi}{\partial\tau}+\frac{\partial}{\partial\zeta}\left(2\frac{Bo}{1+\alpha}\phi^2-\sqrt{\phi}\frac{\partial\phi}{\partial\zeta}\right)=0\,. \qquad (18)$$

2.2 Liquid imbibition into porous substrate

The kinetics of imbibition of a liquid into a porous substrate is described by the Darcy's equation:

$$Q_{pm}=\frac{\kappa}{\mu}\frac{\Delta P}{L} \qquad (19)$$

and

$$\varepsilon\frac{dL}{dt}=\frac{\kappa}{\mu}\frac{\Delta P}{L}\,, \qquad (20)$$

where Q_{pm} is the flux of the liquid inside the porous substrate, ε is the porosity, L is the depth of the wetted part inside the porous layer, κ is permeability of the porous substrate, ΔP is the pressure difference causing the liquid imbibition, according to Eq. (11). Substitution of Eq. (11) into Eq. (20) results in

$$\varepsilon\frac{dL}{dt}=\frac{\kappa}{\mu}\frac{\frac{\gamma}{R_b}\left(4-\frac{C}{\sqrt{C_1\varphi(z=H,t)}}\right)+\frac{n\gamma}{R_{pm}}}{L(t)},\quad L(0)=0\,. \qquad (21)$$

Let us introduce the following dimensionless variables: $l\to L/L_0,\quad \tau\to t/t_0,\quad \phi\to\varphi/\varphi_{cr}$, where L_0 is the characteristic depth of penetration which is defined as:

$$L_0=2\sqrt{\frac{\kappa\gamma t_0}{\varepsilon\mu R_b}(1+\alpha)}\,, \qquad (22)$$

and t_0 and φ_{cr} are defined by Eqs. (16) and (15), respectively. Now Eq. (21) can be rewritten as:

$$\frac{dl}{d\tau}=\frac{\left(1-\frac{1}{\sqrt{\phi(\zeta=1,\tau)}}\right)}{l(\tau)}, \quad l(0)=0. \tag{23}$$

The above dimensionless equation describes the kinetics of liquid penetration into the porous substrate.

2.3 Foam/porous substrate interface

The boundary condition at the foam/porous substrate interface is a mass conservation of the liquid in the case when the free liquid layer does not form:

$$Q_f = Q_{pm}, \tag{24}$$

where Q_f is the flux of liquid from foam to the interface. It can be concluded using Eq. (4):

$$Q_f=\frac{C_1\rho g R_b^2}{3\mu f}\varphi^2(z=H,t)-\frac{\sqrt{C_1}C\gamma R_b}{6\mu f}\sqrt{\varphi(z=H,t)}\frac{\partial\varphi(z=H,t)}{\partial z}. \tag{25}$$

On the other hand, from Eqs. (19) and (11), the flux of liquid from interface into the porous substrate is:

$$Q_{pm}=\frac{\kappa}{\mu}\frac{\frac{\gamma}{R_b}\left(4-\frac{C}{\sqrt{C_1\varphi(z=H,t)}}\right)+\frac{n\gamma}{R_{pm}}}{L(t)}. \tag{26}$$

Substitution of Eqs. (25) and (26) into Eq. (24) results in the following expression for the mass conservation of the liquid at the interface (no free liquid film):

$$\frac{C_1\rho g R_b^2}{3\mu f}\varphi^2(H,t)-\frac{\sqrt{C_1}C\gamma R_b}{6\mu f}\sqrt{\varphi(H,t)}\frac{\partial\varphi(H,t)}{\partial z}=\frac{\kappa}{\mu}\frac{\frac{\gamma}{R_b}\left(4-\frac{C}{\sqrt{C_1\varphi(H,t)}}\right)+\frac{n\gamma}{R_{pm}}}{L(t)}. \tag{27}$$

Using dimensionless variables and co-ordinate as before: $\zeta \to z/H, \quad l \to L/L_0, \quad \tau \to t/t_0, \quad \phi \to \varphi/\varphi_{cr}$, Eq. (27) can be rewritten as:

$$2\frac{Bo}{1+\alpha}\phi^2(1,\tau)-\sqrt{\phi(1,\tau)}\,\frac{\partial\phi(1,\tau)}{\partial\zeta}=\left(\frac{16C_1}{C^2}\right)\varepsilon(1+\alpha)^2\,\frac{L_0}{H}\,\frac{\left(1-\frac{1}{\sqrt{\phi(1,\tau)}}\right)}{l(\tau)}\,. \tag{28}$$

Substituting Eq. (22) into Eq. (28) and introducing Darcy number as:

$$Da=\frac{n^2\kappa}{R_{pm}^2} \tag{29}$$

results in the following dimensionless equation for the conservation of liquid at the interface:

$$2\frac{Bo}{1+\alpha}\phi^2(1,\tau)-\sqrt{\phi(1,\tau)}\,\frac{\partial\phi(1,\tau)}{\partial\zeta}=C_2\sqrt{\varepsilon Da}\,\frac{(1+\alpha)^3}{\alpha}\,\frac{\left(1-\frac{1}{\sqrt{\phi(1,\tau)}}\right)}{l(\tau)} \tag{30}$$

where $C_2=16C_1\sqrt{6f}\big/C^3\sim 2057.8$.

If we adopt the Kozeny-Carman model of the porous substrate as:

$$\kappa=\frac{\varepsilon}{k_z S_{pv}^2} \tag{31}$$

where k_z=2 and S_{pv}=2/R_{pm} for cylindrical pore shape, then Eq. (30) can be rewritten as:

$$2\frac{Bo}{1+\alpha}\phi^2(1,\tau)-\sqrt{\phi(1,\tau)}\,\frac{\partial\phi(1,\tau)}{\partial\zeta}=C_3\varepsilon\,\frac{(1+\alpha)^3}{\alpha}\,\frac{\left(1-\frac{1}{\sqrt{\phi(1,\tau)}}\right)}{l(\tau)} \tag{32}$$

where $C_3=8C_1\sqrt{3f}\big/C^3\sim 727.5$.

The suggested system of equations (18), (23) with boundary condition (32) is valid only when no liquid layer is formed at foam/substrate interface, i.e. if $\varphi(H,t)<\varphi_{\max}$. In this case porous substrate sucks all liquid coming from the foam.

2.4 Accumulation of liquid layer

If the liquid volume fraction at foam/porous substrate interface reaches the maximum limiting value, $\varphi_{\max}$, the accumulation of liquid layer starts (at the moment t=t_m) and free liquid layer is formed in between the porous substrate and the foam. This situation continues until $t=t_M$ when porous substrate sucks the liquid above the layer and again all liquid coming from the foam goes directly into the porous substrate. Therefore, the boundary condition at the bottom of the foam is constant liquid volume fraction at $t_m < t < t_M$:

$$\varphi(H,t) = \varphi_{\max} \tag{33}$$

and in dimensionless form at $\tau_m < \tau < \tau_M$:

$$\phi(1,\tau) = \phi_{\max} \tag{34}$$

where $\varphi_{\max}$~0.26, $\tau_m = t_m/t_0$, $\tau_M = t_M/t_0$ and $\phi_{\max} = \varphi_{\max}/\varphi_{cr}$. The boundary condition (33) or (34) is valid until the moment t_M and afterwards the condition (32) is again satisfied.

In the case of liquid accumulation at foam/porous substrate interface, a mass balance of liquid leads to the following equation for the thickness of film in between the foam and the porous substrate:

$$\frac{dh}{dt} = \frac{C_1 \rho g R_b^2}{3\mu f}\varphi^2(z=H,t) - \frac{\sqrt{C_1}C\gamma R_b}{6\mu f}\sqrt{\varphi(z=H,t)}\frac{\partial\varphi(z=H,t)}{\partial z} - \frac{\kappa}{\mu}\frac{\frac{\gamma}{R_b}\left(4 - \frac{C}{\sqrt{C_1\varphi(z=H,t)}}\right) + \frac{n\gamma}{R_{pm}}}{L(t)}, \tag{35}$$

where h is the thickness of the liquid layer. It is assumed in Eq. (35) that the thickness of liquid layer, $h(t)$, is so small and the pressure inside the film remains constant and is equal to that given by Eq. (10).

We use below the following dimensionless variables and co-ordinate: $\lambda \to h/h_0$, $\zeta \to z/H$, $l \to L/L_0$, $\tau \to t/t_0$, $\phi \to \varphi/\varphi_{cr}$, where h_0 is the characteristic thickness of liquid layer which is determined as:

$$h_0 = \frac{4\kappa\gamma t_0}{\mu R_b L_0}(1+\alpha) = 2\sqrt{\frac{\varepsilon\kappa\gamma t_0}{\mu R_b}(1+\alpha)} = \varepsilon L_0 . \tag{36}$$

Using the above expression, Eq. (35) can be rewritten as:

$$C_3\varepsilon\frac{(1+\alpha)^3}{\alpha}\frac{d\lambda}{d\tau}=2\frac{Bo}{1+\alpha}\phi^2(1,\tau)-\sqrt{\phi(1,\tau)}\frac{\partial\phi(1,\tau)}{\partial\zeta}-C_3\varepsilon\frac{(1+\alpha)^3}{\alpha}\frac{\left(1-\frac{1}{\sqrt{\phi(1,\tau)}}\right)}{l(\tau)}. \quad (37)$$

The suggested system of Eqs. (18), (23) and boundary condition (32) in the case no liquid layer is formed over porous substrate or conditions (32), (34) and (37) in the case of liquid accumulation at the foam-porous substrate interface include three dimensionless parameters: Bo, α (according to Eq. (15)) and the porosity of the porous substrate, ε.

2.4 Model calculation

The model of foam drainage/imbibition described by dimensionless Eq. (18) has been solved below using finite element method on one dimensional regular grid with 50000 elements corresponding to the foam height. The model of liquid imbibition into porous substrate described by Eq. (23) was coupled with foam drainage equation at foam/substrate interface. A backward differentiation formula was used to solve time-dependent variables and time stepping was free taken by solver with initial step size of 10^{-20}. Relative tolerance was set to 10^{-6}, whereas absolute tolerance was set to 10^{-8}. The boundary condition at the top of the foam was zero liquid flux. The boundary condition at foam/porous substrate interface was continuity of flux, Eq. (32), in case no liquid layer is formed over porous substrate or the combination of conditions (32), (34) and (37) in case of liquid layer accumulation. According to Eqs. (18), (23), (32), (34) and (37) kinetics of foam drainage/imbibition depends on three dimensionless numbers: Bo, α and ε. Furthermore, the initial value of liquid volume fraction in foam, $\varphi(z, 0)$, was set to be varied in simulations in order to investigate its effect on the kinetics of foam drainage/imbibition.

3 Results and discussion

The typical dependence of the liquid volume fraction, φ, on the dimensionless foam height, ζ, is shown in Fig. 1 at different times, τ. In the very beginning of the drainage/imbibition the liquid volume fraction decreases only at the top of the foam and near foam/porous substrate interface, whereas in the middle part of the foam the initial value is retained. This is a common feature of foam drainage/imbibition process below. In contrast to the foam placed on a layer of liquid or on a non-porous substrate, the liquid volume fraction at the interface with porous substrate decreases dramatically over a very short time due to imbibition into pores of the porous substrate. After initial considerable decrease in the liquid volume fraction near the interface the difference in the capillary pressure between foam and porous substrate decreases, whereas the penetration depth of the liquid into substrate increases and therefore, according to Eq. (23), the imbibition becomes slower. At the same time there is a continuous supply of liquid to this region from the higher parts of the foam. That is why the further decrease in the liquid volume fractions slows down and in some cases after initial drop; the liquid volume fraction starts to increase and experiences a peak point (see τ=0.002 in Fig. 1). This process is controlled by Bond number, α, ε and initial liquid volume fraction, $\varphi(z, 0)$.

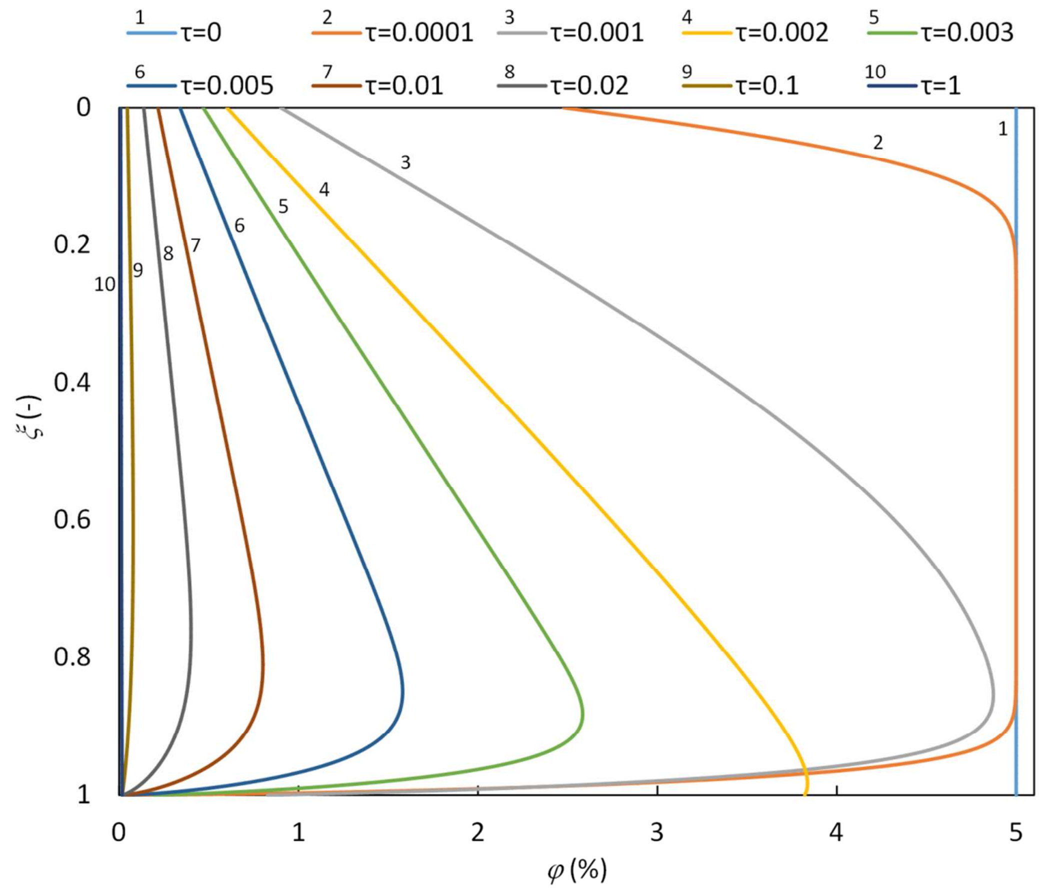

Fig. 1. Time evolution of liquid volume fraction over the foam height at Bo=5.45, α=10, ε=0.03 and $\varphi(z, 0)$= 5%

Fig. 2 shows the time evolution of the liquid volume fraction at foam/porous substrate interface $\varphi(\zeta=1,\tau)$ at various Bo, α and ε numbers, and with various initial liquid volume fractions, $\varphi(z, 0)$. Based on the value of Bo, α, ε and $\varphi(z, 0)$, there are three possible scenarios for the interaction of foam with a porous substrate.

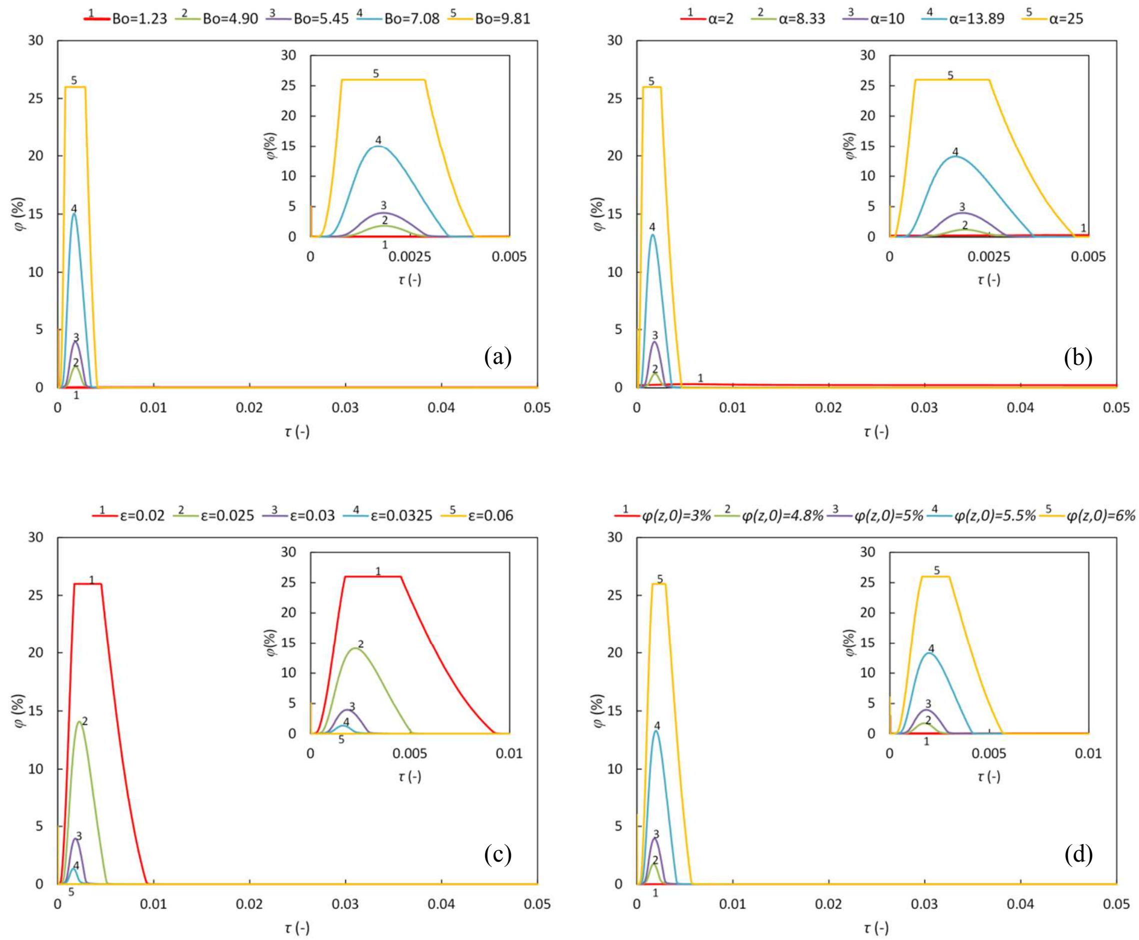

Fig. 2. Time evolution of liquid volume fraction at foam/porous substrate interface at a) α=10, ε=0.03, $\varphi(z, 0)$=5% and various Bo; b) Bo=5.45, ε=0.03, $\varphi(z, 0)$=5% and various α; c) Bo=5.45, α=10, $\varphi(z, 0)$=5% and various ε; d) Bo=5.45, α=10, ε=0.03 and various $\varphi(z, 0)$. In all cases inserts present enlarged region of time scales from 0 to 0.005-0.01. Note, in Fig. 2 the first very fast stage when the liquid volume fraction at the foam/porous substrate interface decreases cannot be clearly shown but it is present in all cases considered.

3.1 Rapid imbibition

As shown in Fig. 2 $\varphi(\zeta=1,\tau)$ is a decreasing function of time at low Bo, α and $\varphi(z, 0)$, and high porosity values, ε (e.g. Bo=1.23 in Fig. 2(a), α=2 in Fig. 2(b), ε=0.06 in Fig. 2(c) and $\varphi(z, 0)$=3% in Fig. 2(d)). In these cases, liquid imbibition into porous substrate occurs quicker as compared with the liquid drainage inside the foam, and liquid volume fraction at the interface does not experience a peak point after initial considerable decrease and it remains constant near final liquid volume fraction. This regime, when the imbibition into porous substrate dominates, is referred to as a *rapid imbibition*.

Fig. 3 shows the time evolution of liquid volume fraction over the foam height at low values of Bo, α and $\varphi(z, 0)$ and high value of porosity, corresponding to the regime of rapid imbibition. Bond number is a ratio of hydrostatic pressure in foam to capillary pressure in bubbles as is defined by Eq. 17. Accordingly, at lower Bond numbers, the capillary forces in foam dominate the gravitational forces acting downward and thus, liquid drainage due to gravity occurs slower than the imbibition into the pores of porous substrate. Therefore, Figs. 1 and 3(a) show the considerable difference: at identical α, ε and $\varphi(z, 0)$, the liquid supply from higher parts of the foam occurs slower at low Bo numbers (Fig. 3(a) as compared with that in Fig. 1). α is a ratio of bubbles radius to the radius of pores according to Eq. 14. At low α numbers, the drainage at the top of the foam proceed slower while the capillary suction imposed by the porous substrate is not considerable also. Therefore, at identical Bo, ε and $\varphi(z, 0)$, the liquid supply from higher parts of foam occurs slower at lower α numbers (Fig. 3(b) as compared with that in Fig. 1). It is also possible to conclude from both Fig. 3(b) and Eq. 15 that final liquid volume fraction is higher at lower values of α. Comparison of Figs. 3(c) and 3(d) with Fig. (1) demonstrates that at higher values of ε and lower values of $\varphi(z, 0)$, the liquid volume fraction at the bottom of the foam does not experience a peak point and it remains constant near final liquid volume fraction.

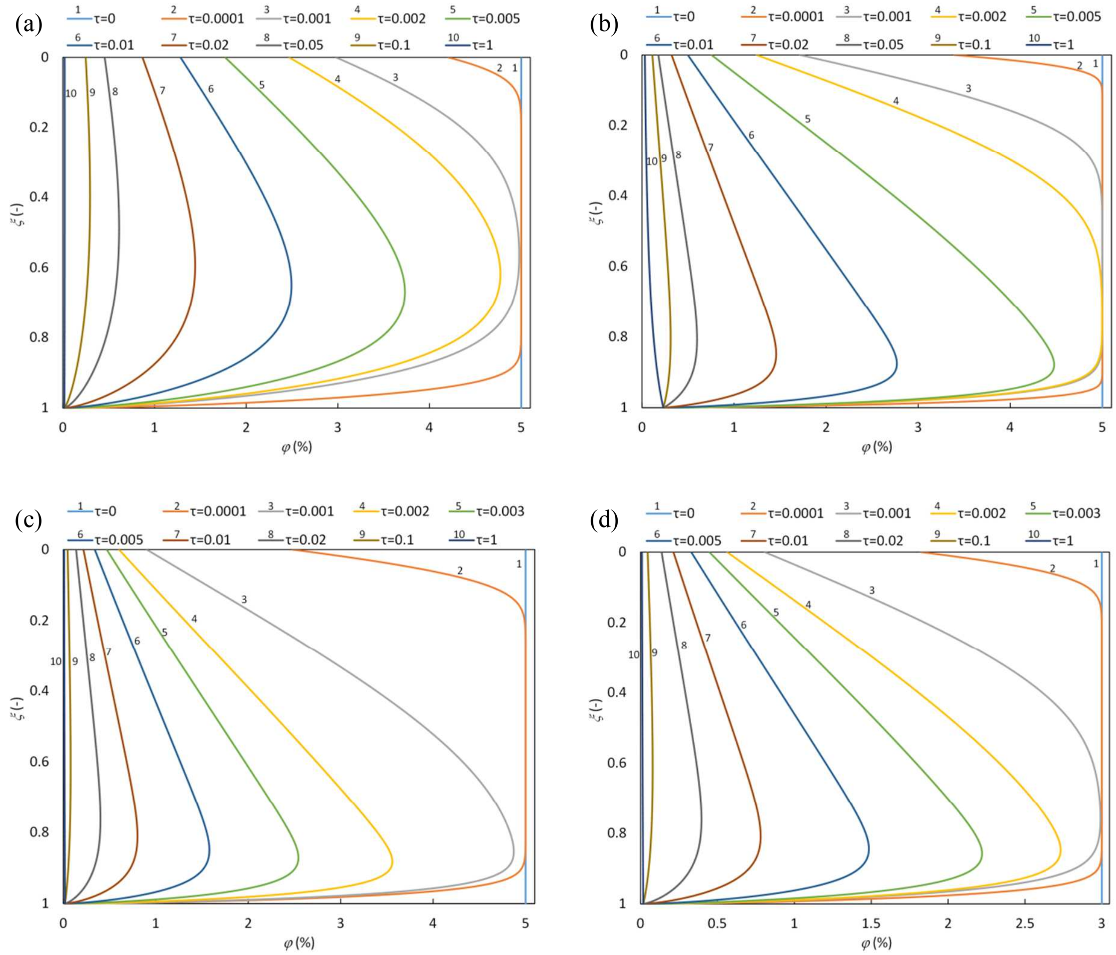

Fig. 3. Time evolution of liquid volume fraction over the foam height at a) Bo=1.23, α=10, ε=0.03 and $\varphi(z, 0)$=5%; b) Bo=5.45, α=2, ε=0.03 and $\varphi(z, 0)$=5%; c) Bo=5.45, α=10, ε=0.06 and $\varphi(z, 0)$=5%; d) Bo=5.45, α=10, ε=0.03 and $\varphi(z, 0)$=3%

In all three plots presented in Figs. 3(a)-3(d) the liquid volume fraction reaches max value somewhere inside the foam, while the liquid volume fraction decreases close both the top and the bottom of the foam. However, there is one important difference between plots presented in Fig. 3(a) as compared with other plots (Figs. 3(b), 3(c) and 3(d)): position of the maximum is close to the middle of the foam on all plots in Fig 3(a) while it is closer to the bottom of the foam in Figs. 3(b), 3(c) and 3(d).

3.2 Intermediate imbibition

Fig. 2 shows that $\varphi(\zeta=1,\tau)$ experiences a maximum value at intermediate Bo, α, ε and $\varphi(z, 0)$ numbers (e.g. Bo=4.90, 5.45 and 7.08 in Fig. 2(a), α=8.33, 10 and 13.89 in Fig. 2(b), ε=0.025, 0.03 and 0.0325 in Fig. 2(c) and $\varphi(z, 0)$=4.8, 5 and 5.5% in Fig. 2(d)). This regime, when the rate of the imbibition into the porous substrate is comparable with the rate of drainage, is referred to as an *intermediate imbibition*. Accordingly, as shown in Fig. 1 the liquid supply from higher parts of foam to the interface occurs quicker, whereas liquid penetration from interface into the porous substrate goes slower at the beginning of the process but the imbibition is faster during the final stage of the process. That is why at the early stage of the drainage/imbibition, liquid volume fraction at the bottom of the foam reaches a maximum value and then it drops to approximately final value. Note that at this regime, there is not any liquid accumulation between the foam and the porous substrate.

3.3 Slow imbibition

The system switched to a different regime at high Bo, α and $\varphi(z, 0)$, and low ε values (e.g. Bo=9.81 in Fig. 2(a), α=25 in Fig. 2(b), ε=0.02 in Fig. 2(c) and $\varphi(z, 0)$=6% in Fig. 2(d)). This regime, when the liquid volume fraction at the foam/porous substrate interface can increase to a maximum limiting value and free liquid layer is formed over the porous substrate, is referred to as a *slow imbibition*.

Fig. 4 shows the time evolution of liquid volume fraction over the foam height in the case of slow imbibition regime, which happens at high values of Bo, α and $\varphi(z, 0)$ and low values of ε, correspondingly. At slow imbibition regime the liquid supply from higher parts of the foam occurs quicker as compared with liquid imbibition into the porous substrate. Accordingly, $\varphi(\zeta=1,\tau)$ reaches the maximum limiting value, $\varphi_{\max}$, at $\tau=\tau_m$ and free liquid layer starts to accumulate between the porous substrate and the foam. Time evolution of the thickness of the free liquid layer is shown in Fig. 5 for Bo=9.81, α=10, ε=0.03 and $\varphi(z, 0)$=5%. The thickness of the free liquid layer increases and reaches a maximum value and then it decreases until the moment $\tau = \tau_M$ when free liquid layer disappears and it is sucked completely by the porous substrate. After that at $\tau > \tau_M$ again all liquid coming from the foam goes directly into the porous substrate and $\varphi(\zeta = 1, \tau)$ also drops to approximately final liquid volume fraction (See Fig. 2).

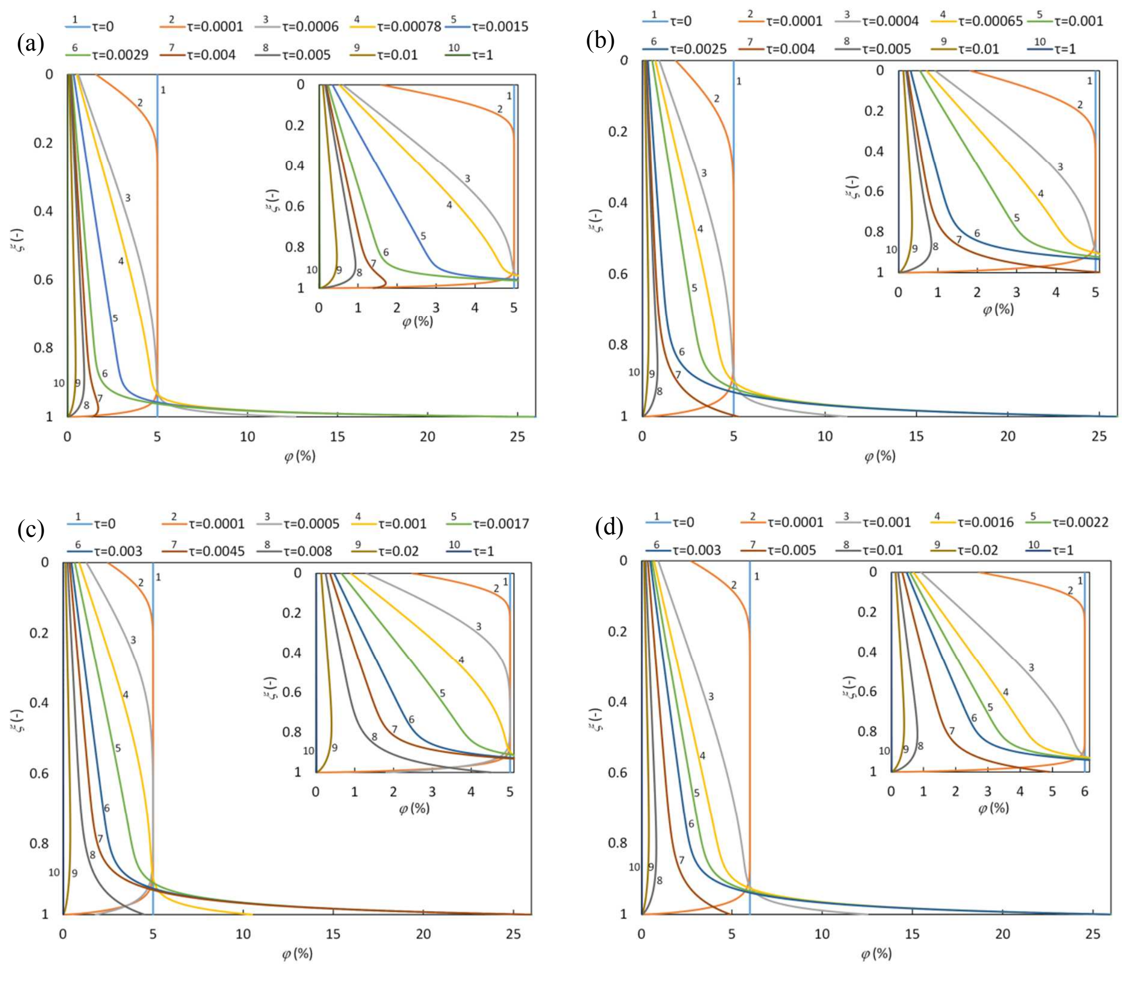

Fig. 4. Time evolution of liquid volume fraction over the foam height at a) Bo=9.81, α=10, ε=0.03 and $\varphi(z, 0)$=5%; b) Bo=5.45, α=25, ε=0.03 and $\varphi(z, 0)$=5%; c) Bo=5.45, α=10, ε=0.02 and $\varphi(z, 0)$=5%; d) Bo=5.45, α=10, ε=0.03 and $\varphi(z, 0)$=6%. In all cases inserts present enlarged region of liquid content from 0 to 5-6%.

Fig. 4 shows that the drainage at the top of the foam is practically uncorrelated with processes near foam/porous substrate interface.

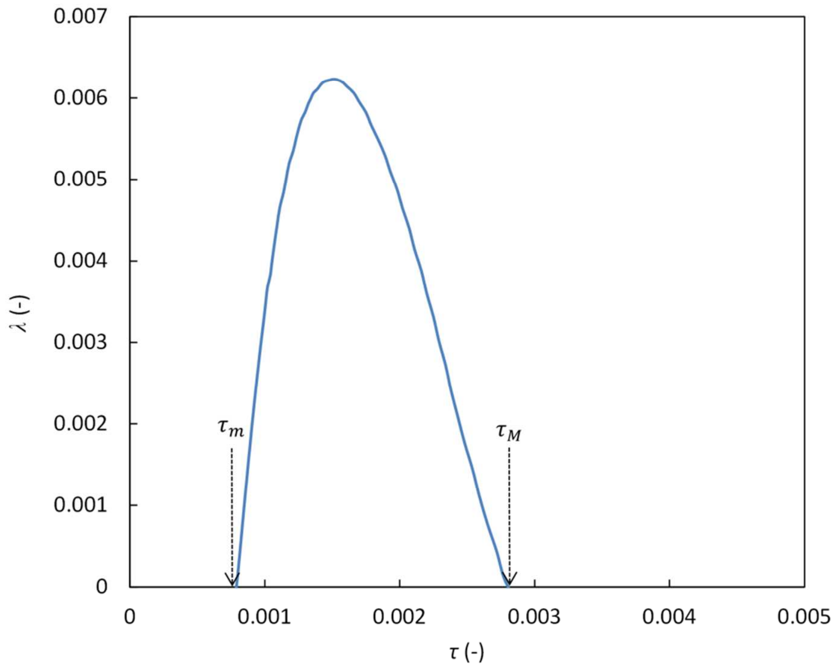

Fig. 5. Time evolution of the thickness of free liquid layer between foam and porous substrate at Bo=9.81, α=10, ε=0.03 and $\varphi(z, 0)$=5% (corresponds to Fig. 4(a)).

Note, there is a difference in time dependencies presented in Fig. 4(a) from those presented in Figs. 4(b)-4(d): at the moment τ=0.004 (just after the free liquid layer disappeared) the dependency of the liquid volume fraction on the foam height has a s-shape character, which is different from all other dependences presented in Figs. 4(b)-4(d).

3.4 Transition points between three regimes of drainage/imbibition

It was shown earlier that the kinetics of foam drainage/imbibition depends on the values of four parameters: Bo, α, ε, and $\varphi(z, 0)$. Below we try to find relations between these four parameters, which determine transitions between three different regimes of the drainage/imbibition process. At a very early stage of the drainage/imbibition, the liquid volume fraction at the foam/porous substrate interface drops from its initial value to roughly final liquid volume fraction and then based on the drainage/imbibition regime it experiences a peak point or remains constant near final value (see discussion of the results presented in Fig. 2). However, even in the fast imbibition regime, there is also a weak peak point, but its value is very close to final liquid volume fraction. If we adopt $\phi(1,\tau)=3$ or $\varphi(H,t)=3\varphi_{cr}$ as a transition point between rapid and intermediate imbibition regimes, using the regression analysis between various simulations we reach the following dimensionless number which determines the boundary between rapid and intermediate imbibition regimes:

$$RI=\frac{Bo^{1.34}\varphi_0^{\ 3.75}}{\varepsilon^{2.56}}\frac{(1+\alpha)^{2.94}}{\alpha}\approx 19\,. \tag{38}$$

If $RI < 19$, then the rapid imbibition regime of drainage/imbibition takes place. According to Eq. (33) a transition between intermediate and slow imbibition regime occurs at $\varphi(H,t)=\varphi_{\max}=0.26$. Therefore, the same procedure as above allows finding another dimensionless number, *IS*, which determine the boundary between intermediate and slow imbibition regimes:

$$IS=\frac{Bo^{1.34}\varphi_0^{\ 3.75}}{\varepsilon^{2.56}}\frac{(1+\alpha)^{2.05}}{\alpha}\approx 35\,. \tag{39}$$

At $IS > 35$, the liquid volume fraction at the foam/porous substrate interface reaches the maximum limiting value and free liquid layer is formed over the porous substrate (slow imbibition). However, at $RI > 19$ and $IS < 35$ the system is in intermediate imbibition regime and no liquid layer is formed at the interface.

4 Conclusions

A model for foam drainage/imbibition placed on a porous substrate was introduced, which allows describing three different regimes of the process. According to suggested mathematical model, kinetics of foam drainage/imbibition depends on three dimensionless numbers: the ratio of capillary pressure in porous substrate to that in bubbles, α, porosity of the porous substrate, ε, Bond number, Bo, and initial liquid volume fraction, $\varphi(z, 0)$. It was found that there are three different regimes of the drainage/imbibition. All three regimes of drainage/imbibition start with a very fast decrease of the liquid volume fraction at the foam/porous substrate interface. All processes are considered after this short initial stage. At low Bo, α and $\varphi(z, 0)$, and relatively high ε values liquid imbibition into the porous substrate occurs faster as compared with the liquid drainage inside the foam. This case was referred to as a *rapid imbibition*. During foam drainage/imbibition at the rapid imbibition regime, the liquid volume fraction at the bottom of the foam remains almost constant close to a final liquid volume fraction after initial considerable decrease. At intermediate Bo, α, ε and $\varphi(z, 0)$ numbers the process of drainage/imbibition switched to a different regime, when the liquid volume fraction at the foam/porous substrate interface experiences a maximum value. At this regime the rates of drainage and imbibition are comparable and this regime is referred to as an *intermediate imbibition*. At even higher Bo, α and $\varphi(z, 0)$, and lower ε values the liquid volume fraction at foam/porous substrate interface increases to a maximum limiting value and free liquid layer is formed over the porous substrate. This case is referred to as a *slow imbibition*. Applying the regression analysis between various simulation results, transition points between three different regimes of drainage/imbibition were determined by introducing two dimensionless numbers.

Acknowledgements

This research was supported by EU CoWet project; Procter & Gamble, USA; EPSRC, UK; PASTA project, European Space Agency; and COST project MP1106.

Nomenclature

A	Plateau border cross-sectional area, m^2
Bo	Bond number
C	geometrical coefficient
C_1	geometrical coefficient
C_2	coefficient
C_3	coefficient
Da	Darcy number
f	drag coefficient
g	gravity acceleration, m/s^2
h	thickness of the free liquid layer, m
h_0	characteristic thickness of the free liquid layer, m
H	foam height, m
k_z	Kozeny constant
l	dimensionless depth of penetration

L	penetration depth, m
L_0	characteristic depth of penetration, m
n	geometrical coefficient of porous substrate
P	pressure, Pa
P_a	atmospheric pressure, Pa
P_b	pressure in a bubble, Pa
P_c	pressure difference in bubble and Plateau border, Pa
P_{pb}	pressure in Plateau border, Pa
P_{pm}	pressure in porous substrate, Pa
Q	flow rate, m^3/s
Q_f	flux of liquid from foam to the foam/porous substrate interface, m/s
Q_{pm}	flux of liquid into the porous substrate, m/s
R_b	radius of bubbles, m
R_{pb}	curvature radius of Plateau border, m
R_{pm}	radius of pores inside porous substrate, m
S_{pv}	specific surface area per unit pore volume, 1/m
t	time, s
t_m	time instant when a free liquid layer starts to form, s

t_M	time instant when a free liquid layer is sucked by the porous substrate, s
t_0	characteristic time scale, s
z	co-ordinate axis, m

Greek Symbols

α	Ratio of capillary pressure in porous substrate to that in bubbles
γ	surface tension, N/m
ε	porosity
ζ	dimensionless vertical co-ordinate
κ	substrate permeability, m^2
λ	dimensionless thickness of the free liquid layer
μ	dynamic viscosity, Pa s
ρ	liquid density, kg/m^3
τ	dimensionless time
τ_m	dimensionless time instant when a free liquid layer starts to form
τ_M	dimensionless time instant when a free liquid layer is sucked
φ	liquid volume fraction
φ_{cr}	final liquid volume fraction
ϕ	dimensionless liquid volume fraction

References

1. D. Exerowa and P. M. Kruglyakov, *Foams and foam films: Theory, experiment, application*, Elsevier, Amsterdam, 1998.

2. S. Farrokhpay, *Advances in Colloid and Interface Science,* 2011, **166**, 1-7.

3. A. Arzhavitina and H. Steckel, *International Journal of Pharmaceutics,* 2010, **394**, 1-17.

4. D. L. Weaire and S. Hutzler, *The physics of foams*, Oxford University Press, Oxford, 1999.

5. A. Saint-Jalmes, *Soft Matter,* 2006, **2**, 836-849.

6. P. M. Kruglyakov, S. I. Karakashev, A. V. Nguyen and N. G. Vilkova, *Current Opinion in Colloid & Interface Science,* 2008, **13**, 163-170.

7. N. Kristen and R. von Klitzing, *Soft Matter,* 2010, **6**, 849-861.

8. P. A. Wierenga and H. Gruppen, *Current Opinion in Colloid & Interface Science,* 2010, **15**, 365-373.

9. S. I. Karakashev and M. V. Grozdanova, *Advances in Colloid and Interface Science,* 2012, **176**, 1-17.

10. R. Farajzadeh, A. Andrianov, R. Krastev, G. J. Hirasaki and W. R. Rossen, *Advances in Colloid and Interface Science,* 2012, **183–184**, 1-13.

11. J. B. M. Hudales and H. N. Stein, *Journal of Colloid and Interface Science,* 1990, **140**, 307-313.

12. M. V. Ramani, R. Kumar and K. S. Gandhi, *Chemical Engineering Science,* 1993, **48**, 455-465.

13. A. R. Bhakta and K. C. Khilar, *Langmuir,* 1991, **7**, 1827-1832.

14. G. Verbist and D. L. Weaire, *EPL (Europhysics Letters),* 1994, **26**, 631.

15. G. Verbist, D. L. Weaire and A. M. Kraynik, *Journal of Physics: Condensed Matter,* 1996, **8**, 3715-3731.

16. S. Jun, D. D. Pelot and A. L. Yarin, *Langmuir,* 2012, **28**, 5323-5330.

17. S. A. Koehler, H. A. Stone, M. P. Brenner and J. Eggers, *Physical Review E,* 1998, **58**, 2097.

18. Q. Sun, L. Tan and G. Wang, *International Journal of Modern Physics B,* 2008, **22**, 2333-2354.

19. D. L. Weaire, N. Pittet, S. Hutzler and D. Pardal, *Physical Review Letters,* 1993, **71**, 2670.

20. S. Hutzler and D. L. Weaire, *Philosophical Magazine Letters,* 2000, **80**, 419-425.

21. P. Stevenson, *Colloids and Surfaces A: Physicochemical and Engineering Aspects,* 2007, **305**, 1-9.

22. S. A. Koehler, S. Hilgenfeldt and H. A. Stone, *Langmuir,* 2000, **16**, 6327-6341.

23. S. A. Koehler, S. Hilgenfeldt and H. A. Stone, *EPL (Europhysics Letters),* 2001, **54**, 335.

24. S. A. Koehler, S. Hilgenfeldt and H. A. Stone, American Physical Society, Division of Fluid Dynamics Meeting, New Orleans, USA, 1999.

25. S. J. Cox and G. Verbist, *Microgravity Science and Technology,* 2003, **14**, 45-52.

26. H. Caps, S. J. Cox, H. Decauwer, D. L. Weaire and N. Vandewalle, *Colloids and Surfaces A: Physicochemical and Engineering Aspects,* 2005, **261**, 131-134.

27. D. L. Weaire, S. Hutzler, G. Verbist and E. Peters, in *Advances in Chemical Physics*, ed. I. Prigogine and S. A. Rice, John Wiley & Sons, Inc., Hoboken, NJ, USA., 1997,.

28. A. Saint-Jalmes, M. U. Vera and D. J. Durian, *EPL (Europhysics Letters),* 2000, **50**, 695.

29. O. Pitois, C. Fritz and M. Vignes-Adler, *Journal of Colloid and Interface Science,* 2005, **282**, 458-465.

30. Y. Zhao, S. A. Jones and M. B. Brown, *Journal of Pharmacy and Pharmacology,* 2010, **62**, 678-684.

31. C. H. Purdon, J. M. Haigh, C. Surber and E. W. Smith, *American Journal of Drug Delivery,* 2003, **1**, 71-75.

32. S. R. Feldman, N. Sangha and V. Setaluri, *Journal of the American Academy of Dermatology,* 2000, **42**, 1017-1020.

33. X. Huang, H. Tanojo, J. Lenn, C. H. Deng and L. Krochmal, *Journal of the American Academy of Dermatology,* 2005, **53**, S26-S38.

34. K. G. Kornev, A. V. Neimark, and A. N. Rozhkov, *Advances in Colloid and Interface Science,* 1999, **82**, 127-187.

35. P. L. Zitha, *Transport in Porous Media,* 2003, **52**, 1-16.

36. K. D. Danov, D. S. Valkovska, and P. A. Kralchevsky, *Journal of Colloid and Interface Science,* 2003, **267**, 243-258.

37. G. Singh, G. J. Hirasaki, and C. A. Miller, *AIChE Journal,* 1997, **43**, 3241-3252.

38. P. L. Zitha, Q. P. Nguyen, P. K. Currie and M. A. Buijse, *Transport in Porous Media,* 2006, **64**, 301-313.

39. P. L. Zitha and F. J. Vermolen, *Transport in Porous Media,* 2006, **63**, 195-200.

40. A. Bureiko, O. Arjmandi-Tash, N. Kovalchuk, A. Trybala and V. M. Starov, *The European Physical Journal Special Topics,* 2015, in press.

41. F. Bolton and D. L. Weaire, *Physical Review Letters,* 1990, **65**, 3449-3451.

42. M. Van Hecke, *Journal of Physics: Condensed Matter,* 2010, **22**, 033101.

43. P. Grassia, J. Cilliers, S. Neethling and E. Ventura-Medina, *The European Physical Journal E,* 2001, **6**, 325-348.

Graphical Abstract

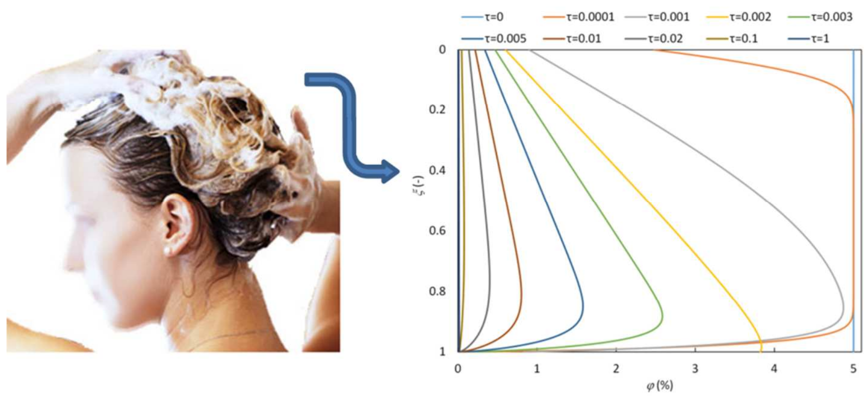

Direct numerical simulations were performed to identify the kinetics of liquid release from a foam into a porous substrate like a skin or a bunch of hair.